High-Gain Cuk DC-DC Converter with Switch-Capacitor and Switched Inductor: A Non-Isolated Design

A. Clement Raj
Department of Electrical Engineering, Faculty of Engineering and Technology, Annamalai University

R. Bens Raj
Department of Electrical Engineering, Faculty of Engineering and Technology, Annamalai University

https://doi.org/10.5109/7160912

出版情報：Evergreen. 10 (4), pp.2339-2352, 2023-12. 九州大学グリーンテクノロジー研究教育センター
バージョン：

High-Gain Cuk DC-DC Converter with Switch-Capacitor and Switched Inductor: A Non-Isolated Design

A. Clement Raj[1,*], R. Bens Raj[1]

[1]Department of Electrical Engineering, Faculty of Engineering and Technology, Annamalai University, Chidambaram 608002, Tamil Nadu, India

*Author to whom correspondence should be addressed:
E-mail: clementlecturer1@gmail.com, clementlecturer@gmail.com

(Received August 27, 2023; Revised October 12, 2023; accepted October 17, 2023).

Abstract: This work introduces the DC-DC topology of a non-isolated high-gain step-up Cuk converter. The proposed topology is based on implementing switched-capacitor (SC) and switched-inductor (SL) techniques. The primary focus of this topology is the application in renewable energy systems and electric vehicles, specifically in photovoltaic and fuel cell technologies. The proposed topology exhibits a notable enhancement in voltage boost capability when compared to the traditional boost and Cuk converters, owing to the implementation of SC and SL approaches. The suggested Cuk converters are obtained by modifying the original Cuk converter, wherein the single inductor present at the output and input sides is substituted with an SL, and the energy-transferring capacitor is replaced with an SC. The primary benefits of the recommended Cuk converters lie in their ability to achieve a high output voltage gain and mitigate the voltage stress experienced by the power switch. Hence, it is possible to utilize a MOSFET with a lower voltage capacity, resulting in a lesser $R_{ds\text{-}ON}$ and increasing efficiency. A comparison has been made between the voltage gain and voltage stress across the primary switch in the proposed converter and the Cuk and boost converter. The recommended topology is intended to circumvent the need for a transformer, coupled inductors, or severe duty cycles. This design approach results in reduced volume, loss, and cost. The proposed converter is evaluated under the continuous conduction mode. The present study provides a theoretical investigation of the continuous conduction mode, whereby all relevant expressions are derived and compared with the corresponding simulation results.

Keywords: Cuk converter; DC-DC conversion; Switch-capacitor; Switch-inductor

1. Introduction

The power converters play a vital role as essential components in a wide range of applications. Upon closer examination of their significance, it becomes evident that they possess an inherent indispensability across multiple domains. The power converters play a critical role in operating systems that utilize solar, wind, and other forms of renewable energy[1,2]. Renewable sources often generate variable voltage inputs, and power converters play a crucial role in transforming these inputs into a stable and usable voltage output, thereby maximizing energy utilization. DC-DC converters are significant in hybrid vehicles, combining conventional fuel and electric propulsion, and fully electric vehicles (EVs), which solely rely on electric power[3-5]. These components are responsible for facilitating the effective transmission of power from the battery to the diverse electronic systems and motors of the vehicle, thereby enhancing the overall performance of the vehicle[6,7]. The utilization of microgrids in power systems. Microgrids are characterized as smaller-scale energy grids that are localized in nature. These microgrids prominently depend on the utilization of DC-DC converters[8]. These converters optimize power distribution within the grids, ensuring a consistent power supply even during main grid failures. Voltage regulation applications refer to the various uses and implementations of voltage regulation techniques. Numerous electronic devices and systems must maintain consistent voltage levels to ensure reliable functionality[9]. DC-DC converters assume a crucial function in preserving these voltage levels, thereby ensuring the protection of devices against possible voltage fluctuations[10]. These converters can be classified into two primary types: (i) Linear Converters functions based on utilizing linear passive components, such as resistors, arranged in series or shunt configurations[11]. The principal benefits of linear converters encompass their inherent simplicity and capacity to generate output voltage with negligible noise interference. However, they are not devoid of limitations. The utilization of passive components inherently results in power losses caused by heat dissipation, thereby reducing the overall efficiency of the converter. The phenomenon of energy loss assumes particular significance in systems that require a high-power

throughput. Furthermore, it should be noted that linear converters have a predominant operational scope focused on voltage reduction, also known as stepping-down, and (ii) Switching converters refer to a type of electronic device that is used to convert electrical energy from one form to another[12,13]. These converters are commonly employed in various applications, such as switching converters utilizing at least one semiconductor-controlled switch to control and regulate the output voltage effectively. One noteworthy advantage of these converters is their inherent versatility, as they can be engineered for various purposes, including voltage step-up, step-down, and polarity inversion. This adaptability enables them to cater to a broader spectrum of applications. The incorporation of controlled switches, although contributing to the complexity of the system and the potential generation of output noise, significantly enhances the converter's efficiency. The aforementioned high efficiency renders them the favoured option for many applications, notwithstanding the increased intricacy[14,15]. The selection between linear and switching converters is contingent upon the specific demands of a given application, necessitating a careful evaluation of the compromises between simplicity, noise, and efficiency[16].

In the current context, excessive utilization of petroleum-based fuels in automobiles has released greenhouse gases and other harmful substances. Consequently, this has resulted in substantial environmental risks, health concerns, and price volatility. In recent decades, EVs and electric hybrid vehicles (EHV) have emerged as viable options for inter-city transportation. These vehicles provide numerous advantages, including low maintenance requirements, great efficiency, decreased noise and environmental pollution, and economic effectiveness[17,18]. In powering EVs and EHVs, pollution-free battery power has become the most favoured energy source. This particular energy source is rechargeable at dedicated battery charging places[19,20]. Nevertheless, due to the rapid development anticipated in the EV sector, power quality issues likely arise within the current electrical networks. Given the widespread adoption of power electronics systems in battery recharging points, there has been a growing worry regarding power quality issues, specifically harmonic pollution in the distribution network[21,22]. Implementing battery charging stations in metropolitan areas has led to an elevated danger of harmonic levels in energy distribution networks, thereby diminishing the lifespan of distribution transformers. Traditionally, a diode rectifier, accompanied by a large filter capacitor, generates a supply current is extremely distorted, non-sinusoidal, and characterized by peaks. This current exhibits a high total harmonic distortion (THD) of approximately 70-80%. Moreover, it is drawn from a single-phase source with a low power factor ranging from 0.75 to 0.8, which is lagging. Additionally, the current has a high crest factor[23]. According to internationally recognized Power Quality (PQ) standards such as IEEE Standard 519-1992 and IEC 61000-3-2, it is increasingly important for any product to meet the power factor requirement of 0.9 and above, and maintain a current THD under 5% for Class-D applications[7, 8].

To adhere to the established global norms about Power Quality (PQ), many ac-dc converter designs have been extensively documented in scholarly literature. Two-stage power factor correction (PFC) converters are primarily employed[24]. The initial phase of these designs is specifically focused on power factor correction, whereas the subsequent phase is responsible for voltage or current stabilization. The design selection for the latter stage can be determined according to specific requirements. Furthermore, it should be noted that PFC converters, whether isolated or non-isolated, can operate in either a continuous or a discontinuous conduction mode[25]. Nevertheless, one limitation of these dual-stage designs is their less-than-optimal efficiency, further compounded by the requirement for many components. Although cost-effective designs can be found in academic studies, it is rare to come across highly efficient single-stage converters suitable for low-power applications. Several scholarly works have presented innovative single-stage PFC designs that utilize a single active switch and control circuit. These designs effectively handle both output voltage stabilization and input current modulation simultaneously. Nevertheless, one of the primary obstacles associated with these designs is the notable voltage strain exerted on the switch, which experiences fluctuations due to input voltage changes and output load modifications. When employed in conjunction with universal input sources, the voltage encountered by components can potentially exceed 450V[26]. Therefore, it is imperative to develop semiconductor devices with elevated voltage ratings and significant capacitance, particularly when confronted with wide-ranging variations in input voltage. Suggestions have been made to alleviate the voltage strain on components[27]. However, the attainment of low output voltages and the reduction of voltage stress may require the utilization of a transformer. In cases where it is unnecessary, including galvanic isolation incurs supplementary expenses.

Switching converters, a cornerstone in modern power electronics, can be broadly classified into two categories: soft-switching and hard-switching resonant converters. The non-isolated hard-switching resonant converters do not employ any form of galvanic isolation. Examples include Boost, Buck, Buck-Boost, SEPIC, and Cuk converters[28-30]. Structurally, these converters commonly comprise a controlled MOSFET switch, an individual diode, one or occasionally two inductors, and a filter to reduce high-frequency noise and voltage spikes. Isolated hard-switching converters are distinctly different from their non-isolated counterparts, and these converters incorporate galvanic isolation mechanisms. The inclusion of equipment such as transformers is what differentiates them. For instance, a flyback converter, as discussed, and a forward converter both employ a transformer to achieve this isolation. However, hard-switching converters inherently have a limitation: they tend to exhibit high switching losses. This factor detrimentally affects their efficiency, especially at higher operating frequencies[31].

The soft-switching resonant converters overcome the challenges posed by the high switching losses of hard-switching converters. These converters have been ingeniously designed to minimize switching losses, enhancing efficiency. They can be categorized into zero voltage switching (ZCS) and zero current switching (ZVS) converters. The designs capitalize on the principle that switching losses can be considerably reduced when transitions occur at either zero current (in ZVS) or zero voltage (in ZCS)[32,33].

With the surging interest and development in renewable energy sources, particularly solar and wind energy, there is an escalating need for DC-DC converters that can invert output voltage. In hybrid systems that integrate solar and wind power, maintaining a consistent voltage source becomes pivotal, especially during instances when solar intensity diminishes or wind speed drops below optimal levels, as highlighted in reference[34,35]. The EVs present another intriguing application. An EV typically incorporates two energy storage units: a primary source offering large energy storage and a secondary, rechargeable storage arrangement facilitating bi-directional power flow[36,37]. In such scenarios, a converter with an inverted output voltage is imperative. Converters such as the Cuk and the buck-boost converters are particularly favoured in these applications because they produce an inverted output voltage, as emphasized in reference[38-40].

The Buck-Boost converter can manipulate the output voltage by either increasing or decreasing it while employing a limited number of components. One significant benefit of this converter is its notable efficiency, achieved by operating at a reduced duty cycle. This characteristic makes it a feasible option for many applications[41]. However, there are certain constraints associated with it. The pursuit of increased gains frequently entails a compromise in terms of efficiency. The potential instability of the Buck-Boost converter in certain situations can be attributed to its inherent lack of isolation[42]. Furthermore, if the integrated switch remains OFF, the energy stored in the inductor is reflected to the source. The abovementioned behaviour may be deemed unfavourable and potentially restrict the converter's efficacy[41]. In contrast, the Cuk converter demonstrates proficiency in amplifying and attenuating the output voltage. Incorporating two inductors in its design facilitates the reduction of fluctuations in both input and output currents. Moreover, it is distinguished by its perpetual influx and efflux of electrical current. In the operational process of the Cuk converter, upon the closure of the switch, the intermediary capacitor facilitates the transfer of energy to the output inductor L2 and the subsequent load. In contrast, when the MOSFET is deactivated (opened), the stored energy within L2 is exclusively directed towards the load[9,43]. Nevertheless, there are certain challenges associated with this. In certain cases, the integration of a compensatory circuit into the Cuk converter may be undertaken in order to ensure stability. The inclusion of this additional component has the potential to impede the system's ability to respond promptly. After a comprehensive evaluation of the literature on DC-DC converters, the authors affirm that the proposed configuration has not been previously reported. Therefore, this study presents a new converter configuration validated through computer simulations. The derived configuration enhances operational efficiency while concurrently minimizing the voltage requirement of the coupling capacitor.

In this study, we present an integration of switched-inductor (SL)[44,45] and switched-capacitor (SC)[46,47] methodologies into the traditional Cuk converter[48-49], leading to the development of new enhanced high gain Cuk converters. The motivation for selecting the Cuk converter stems from its unique advantages in certain applications, such as its non-inverted output, continuous input and output currents, and its capability for both step-up and step-down voltage conversions. It is also observed that while the Cuk converter has these advantages, there is potential to further improve its performance, especially in terms of efficiency and transient response. This study aimed to address these performance aspects, making the Cuk converter even more appealing for a wider range of applications. When observing from the circuit design perspective, combining SL and SC within the Cuk converter framework results in a distinct converter variant that deviates from existing Cuk converters. The primary benefits of the newly proposed converters can be outlined as:

- Facilitation of a non-isolated voltage transition path from negative to positive, grounded in relation to a standard reference.
- Achievement of superior voltage conversion metrics compared to traditional Cuk and boost converters, a feat made possible through the innovative SL and SC methods.
- Reduction in voltage strain experienced by the principal switch when contrasted with traditional Cuk and boost converters. This paved the way for the employment of a switch characterized by a diminished voltage rating and reduced R_{ds-ON}.
- Regarding the unique design, additional components comprising a set of diodes, a capacitor, and inductors are integrated into the Cuk converter. This facilitates the execution of SL and SC processes, aiming to augment voltage gain.
- Retention of a single-switch mechanism.
- Preserving a key feature intrinsic to the classical Cuk converter, the continuous flow of current at both input and output terminals, enabled by respective input and output inductors, remains intact in the devised topologies.

The traditional and proposed Cuk converter is comprehensively discussed in Section 2. Section 2 delves into the power circuit, its operational modes, and an in-depth analysis of the circuit. In Section 3, the suggested Cuk topology is contrasted with the traditional Cuk converter, the boost converter and modified Cuk converter

versions, focusing on voltage gain and switch voltage stress. Section 4 presents and discusses the results. Section 5 wraps up with a summary and a conclusion, also touching upon potential future directions for the proposed converter.

2. Proposed SCSL-Based Cuk Converter

This section briefly discusses the operation of the traditional Cuk converter. Then, the operation and circuit analysis of the proposed SLSC-based Cuk converter are discussed.

2.1. Traditional Cuk Converter

As depicted in Figure 1, the traditional Cuk converter and buck-boost converter are both DC-DC converters. These converters are designed to generate an output voltage magnitude that can be either higher or lower than the input voltage[48,49]. A unique feature of these converters is their ability to invert the polarity of the output voltage. The rationale behind this functionality is rooted in their inherent voltage conversion ratio, as elaborated in Eq. 1.

$$A_{Cuk} = A_{Buck-Boost} = \frac{V_{out}}{V_{in}} = -\frac{D}{1-D} \quad (1)$$

where A_{Cuk} and $A_{Buck-Boost}$ denote the voltage gain of the Cuk converter and buck-boost converter, respectively, V_{out} denotes the output voltage of the converter, V_{in} denotes the input voltage of the converter, and D denotes the duty cycle of the power switch.

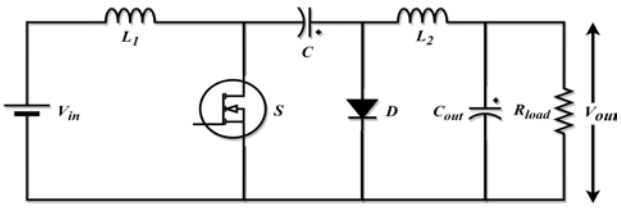

Fig. 1. Circuit diagram of the traditional Cuk DC-DC converter.

A critical parameter in the operation of these converters is the duty cycle. The magnitude of this duty cycle plays a pivotal role in dictating the performance of these converters. It can pose challenges if the duty cycle becomes exceedingly high, especially values nearing or exceeding 0.9. The primary reason for this limitation is the influence of parasitic components, which can adversely impact the converter's efficacy[19]. Diving deeper into the classical Cuk converter, it operates through three distinct modes, namely: (i) boost mode, (ii) buck mode, and (iii) buck-boost mode. The Cuk converter is lauded for several inherent advantages, which include (i) The presence of an energy transfer capacitor, which plays a crucial role in its operation; (ii) Exceptional steady-state performance, ensuring consistency in its functioning; (iii) A consistent flow of current at both the input and output terminals, meaning both currents are continuous, and (iv) Minimal ripples in the output voltage, ensuring a smoother voltage output.

2.2. Research Motivations

Like many converters, the traditional Cuk converter has its advantages but comes with challenges or problems. As discussed earlier, the duty cycle cannot achieve extremely high values, especially nearing or exceeding 0.9[34,35]. This limitation can hinder the converter's boost voltage capabilities. Parasitic components can adversely impact the performance of the Cuk converter. These unwanted components, such as stray inductances and capacitances, can introduce inefficiencies, energy losses, or even operational instabilities. The Cuk converter's design and operational modes are more complex than simpler converters like the buck or boost. This complexity can make its implementation and troubleshooting more challenging. As found in certain literature, some modified versions or variants of the Cuk converter have a low voltage conversion ratio. This can limit their effectiveness in applications that require a high conversion ratio. The Cuk converter design can sometimes expose certain components, like capacitors and inductors, to higher stresses, especially during transient conditions or under specific load scenarios. Due to its inherent design, which often includes multiple inductors, capacitors, and switches, the Cuk converter might be bulkier and more expensive than other simpler converter alternatives. Achieving desired performance specifications, like output voltage regulation or transient response, might require sophisticated control strategies, adding to the overall system complexity. After thorough investigations, it is identified that there is a need for an advanced Cuk converter topology for the higher voltage gain with lower voltage stress. This motivated this study to propose a converter topology based on the Cuk converter with boosting methods, such as SL and SC.

2.3. SCSL-Based Cuk Converter Topology

The development of the SCSL-based Cuk converter is based on the original Cuk converter design. In this particular modification, the inductor located on the input is replaced with a switched inductor, whereas the energy-transfer capacitor is substituted with an SC. The schematic of the proposed converter is illustrated in Fig. 2. Compared to the Cuk design, the proposed model depicted in Fig. 2 integrates an extra inductor, capacitor, and four diodes.

2.3.1. Modes of operation

This study delves into a detailed analysis and description of the operation of the proposed SCSL-Based Cuk converter under Continuous Conduction Mode (CCM). The CCM describes a scenario in power electronics where current continuously flows through an inductor. The functioning of the proposed converter can be better understood when looked at in two primary operating modes based on the state of the power

semiconductor switch, i.e., (i) ON-mode: S is conducting (turned on) and (ii) OFF-mode: S is not active (turned-off).

When the MOSFET S is actively conducting or turned on, it allows for current flow in a certain direction, as depicted in Fig. 3a. The input supply voltage, denoted by V_{in}, charges the inductors L1 and L2 in parallel. This charging action occurs through diodes $D1$, $D3$, and, most importantly, through the conducting switch S. Diodes $D2$, $D4$, and $D5$ are in a state known as reverse-biased during this mode.

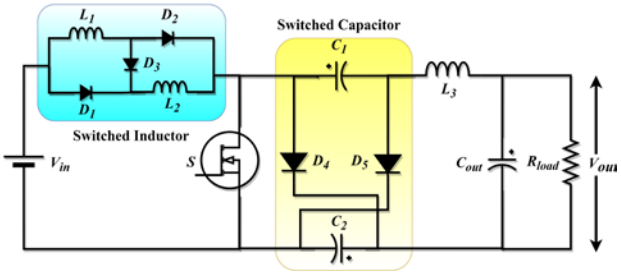

Fig. 2. Proposed SCSL-based Cuk DC-DC converter topology

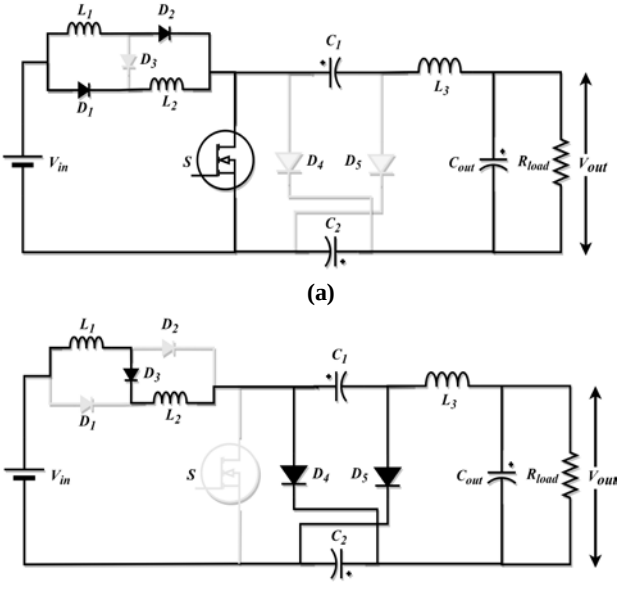

(a)

(b)

Fig. 3. Mode of Operation: (a) ON-state, (b) OFF-state

Being reverse-biased means they block current flow in the direction they are oriented. The source voltage V_{in} collaborates with the energy stored in $C1$ and $C2$ to deliver power to the load. This combination also charges the inductor $L3$ with the assistance of the conducting switch. A notable characteristic is that equal amounts of current flow through the L1 and L2. This uniformity is because both inductors share identical specifications.

In contrast to the ON-Mode, when the switch is not active or turned off, the current flows in a direction shown in Fig. 3b. The energy stored in the inductors L1 and L2 due to the input supply voltage V_{in} now charges the $C1$ and $C2$. These capacitors are associated in parallel. Similarly, the stored energy in inductor L3 charges $C1$ and $C2$ and also delivers power to the load. During this mode, diodes $D1$ and $D3$ become reverse-biased. Finally, to give a graphical representation and to tie all these functional descriptions together, Fig. 4 provides a visual portrayal of the switching diagrams. These diagrams display the steady-state waveforms associated with CCM and highlight significant variations specific to the proposed converter. This comprehensive description breaks down the functionalities of the proposed converter in CCM.

2.3.2. Circuit analysis

For a clearer understanding, start with the premise that the suggested converter is operated in a steady-state mode[2,9]. This approach aids in streamlining the evaluation. A few foundational assumptions to take note of include:

- Every component functions perfectly with a 100% efficiency.
- The input voltage is purely direct current.
- All the capacitors are designed to ensure a minimal voltage fluctuation at the switching frequency.

When the switch is in the active or conducting state, the voltage levels across L1, L2, and L3 can be described as per Eqs. 2-3. For clarity, assume that the capacitor values of C1 and C2 are the same, i.e., $C1 = C2 = C$.

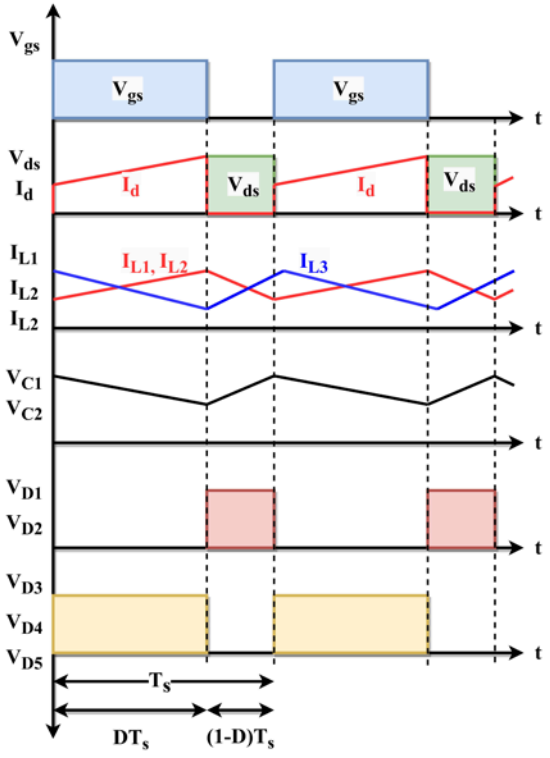

Fig. 4. Theoretical waveforms of the proposed converter

$$V_{L_1} = V_{L_2} = V_{in} \quad (2)$$

$$V_{L_3} = 2V_C - V_{out} \quad (3)$$

When the MOSFET is inactive or turned off, the voltage levels across L1, L2, and L3 can be described as per

Eqs. 4-5. For clarity, assume that the capacitor values of C1 and C2 are the same, i.e., C1 = C2 = C.

$$V_{L_1} = V_{L_2} = \frac{V_{in}-V_C}{2} \quad (4)$$

$$V_{L_3} = V_C - V_{out} \quad (5)$$

The following equations are obtained by applying the volt-second balance principle.

$$V_{in}D + (1-D)\left(\frac{V_{in}-V_C}{2}\right) = 0 \quad (6)$$

$$D(2V_C - V_{out}) + (V_C - V_{out})(1-D) = 0 \quad (7)$$

Now, the voltage across the capacitors C1 and C2 are calculated as follows.

$$V_{C1} = V_{C2} = V_C = \frac{(D+1)}{(1-D)}V_{in} \quad (8)$$

Finally, the ideal voltage gain of the proposed converter A_{CCM} is given as follows.

$$A_{CCM} = \frac{V_{out}}{V_{in}} = \frac{(D+1)^2}{(1-D)} \quad (9)$$

Referring to Figs. 3a and 3b, one can derive a formula to determine the current for the pair of input inductors. Given that both input inductors possess identical inductance, the equation $I_{L1} = I_{L2} = I_{Lin}$ can be deduced from Eq. 10, as illustrated in Eq. 11.

$$I_{in} = 2DI_{L_{in}} + (1-D)I_{L_{in}} \quad (10)$$

$$I_{L_{in}} = \frac{I_{in}}{(D+1)} = \frac{P_{out}}{V_{in}(D+1)} \quad (11)$$

The capacitor C_{out} functions as a low-pass filter. Consequently, from this, the equation $I_{L3} = I_{Lout}$ can be inferred as shown in Eq. 12.

$$I_{L_{out}} = I_{out} = \frac{P_{out}}{V_{out}} \quad (12)$$

The opposing voltage on $D1$ and $D3$ when they are in the non-conducting or OFF state is depicted in Eq. 13.

$$V_{D_1} = V_{D_3} = \frac{D}{(1-D)}V_{in} \quad (13)$$

When $D2$ is in its conducting or ON state, the counteracting voltage is represented in Eq. 14.

$$V_{D_2} = V_{in} \quad (14)$$

The counter voltage on $D4$ and $D5$ of the switched capacitor, when they are in the conducting or ON state, is articulated in Eq. 15.

$$V_{D_4} = V_{D_5} = \frac{(1+D)}{(1-D)}V_{in} \quad (15)$$

The voltage strain on the power switch when it is in the non-conducting or OFF state is outlined in Eq. 16.

$$V_S = \frac{(1+D)}{(1-D)}V_{in} \quad (16)$$

The capacitor's voltage exhibits a peak-to-peak shift, denoted by $\triangle v_{C1} = \triangle v_{C2} = \triangle v_C$, as highlighted in Eq. 17.

$$\triangle v_C = \frac{DTI_{out}}{C} = \frac{DP_{out}}{A_{CCM}V_{in}fC} \quad (17)$$

The variations in current for the inductors at the input are represented as $\triangle i_{L1} = \triangle i_{L2} = \triangle i_{Lin}$, and at the output, indicated by $\triangle i_{L3} = \triangle i_{Lout}$, can be found in Eqs. 18-19.

$$\triangle i_{L_{in}} = \frac{DTV_{in}}{L_{in}} = \frac{DV_{in}}{fL_{in}} \quad (18)$$

$$\triangle i_{L_{out}} = \frac{DT(2V_C - V_{out})}{L_{out}} = \frac{D(2V_C - V_{out})}{fL_{out}} \quad (19)$$

3. Performance Comparison

In a detailed examination of various converter topologies, this study contrasted the proposed Cuk topology with their more traditional counterparts: the classical Cuk[48,49], boost[50], Modified Cuk 1[43], and Modified Cuk 2[51] converters. This comparison is meticulously laid out in Table 1 for easy reference and analysis. Delving into the specifics, the proposed SCSL-based Cuk converter topologies outperform the classical versions regarding voltage gain. This essential means that the new topologies can convert a given input voltage to a significantly higher output voltage. The proposed SCSL-based Cuk topology stands out as the pinnacle in terms of voltage gain. To provide a clearer and more visual understanding of this superior performance, a graphical representation has been provided in Fig. 5a.

Beyond the sheer voltage gain, another critical factor in the performance and reliability of these topologies is the voltage stress they exert on the components. Specifically, we look at the normalized voltage, denoted as V_S/V_{in}, on the main switch. This metric offers insights into the voltage stress experienced by the semiconductor device, in this case, the MOSFET. High voltage stress can lead to premature wear and potential failure of the component, so a lower value is usually more desirable.

Table 1. Performance comparison between various converter topologies

Topology	Cuk	Boost	Modified Cuk 1	Modified Cuk 2	Proposed
MOSFETs	1	1	1	2	1
Diodes	1	1	3	2	5
Capacitors	2	1	3	3	3
Inductors	2	1	2	3	3

Voltage Stress	$\frac{D}{1-D}$	$\frac{1}{1-D}$	$\frac{D}{(1-D)^2}$	$\frac{1}{(1-D)^2}V_{in}$	$\frac{(1+D)}{(1-D)}V_{in}$
Voltage Gain	$\frac{D}{1-D}$	$\frac{1}{1-D}$	$\frac{D}{(1-D)^2}$	$\frac{D(2-D)}{(1-D)^2}$	$\frac{(1+D)^2}{(1-D)}$

To provide a comprehensive understanding, the normalized voltage values for the proposed converter have been contrasted with those from the classical Cuk converter and their modified versions and boost converter. Once again, this comparison has been graphically visualized in Fig. 11b for a more intuitive grasp. The proposed Cuk topology manifests lower voltage stress than the traditional designs, but among them, the proposed converter emerges as the clear winner, exerting the least voltage stress on its components.

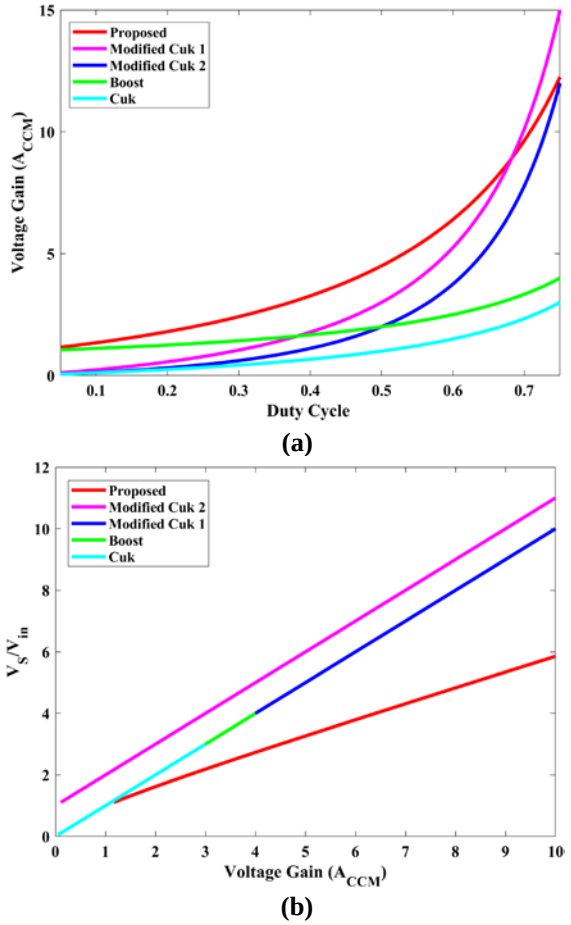

Fig. 5. Performance comparison: (a) Voltage gain, (b) MOSFET voltage stress

4. Results and Discussion

The proposed SCSL-based Cuk DC-DC converter is designed for a source voltage of 24V with a capacity of 200W, a switching frequency of 75 kHz, and the duty cycle of the MOSFET switch is 65%. The proposed converter is developed and tested using the MATLAB/SIMULINK software. The electrical specifications of the SCSL-based Cuk converter topology are listed in Table 2.

Table 2. Electrical specifications of the recommended Cuk converter

S. No.	Parameters	Specifications
1.	Source voltage V_{in}	24 V
2.	Power output P_{out}	200 W
3.	Output voltage V_{in}	186 V
4.	Duty cycle D	0.65
5.	Switching frequency f_s	75 kHz
6.	Capacitors (C_1 and C_2)	47 μF
7.	Inductors (L_1, L_2, and L_3)	440 μH
8.	Load resistance R_L	173 Ω

The proposed SCSL-based Cuk converter has been meticulously designed to deliver an output voltage of approximately -186 V. A graphical representation captures the voltage and current stresses experienced by the MOSFET. The visual aids in understanding the peaks and troughs of these stresses during the operational cycle. The current and voltage stresses on the MOSFET are illustrated in Fig. 6a. The stresses MOSFET undergoes during operation are critical determinants of its efficiency and longevity. Specifically, the peak value of the voltage stress on this MOSFET is around 84 volts. Concurrently, the peak value of the current stress measures at about 13.2 amperes.

A common arrangement in the SL cell involves three diodes, which help achieve high output voltage levels depending on the switching devices' configuration and state. The switched inductor cell has three diodes (D1, D2, and D3) and two inductors. When the switching device is ON, the inductor is charged. This is similar to the boost converter operation. When the switching device is OFF, the inductor discharges, transferring energy to the load and/or back to the source. When the MOSFET switch is active, D1 is reverse-biased as the inductor is getting charged. Thus, the voltage across D1 is negative (the voltage source and the state of inductor charging determine the magnitude), as shown in Fig. 7a. When the MOSFET switch is inactive, D1 becomes forward-biased and conducts, allowing the inductor to discharge. The voltage across D1 drops to zero or near zero. When the switch is active, D2 is reverse-biased. The voltage across D2 is the sum of the inductor voltage and the output voltage, resulting in a high negative voltage, as shown in Fig. 7b. When the MOSFET switch is OFF: If the inductor voltage exceeds the output voltage, D2 becomes forward-biased and conducts. The voltage across D2 is near zero during this interval. When the MOSFET switch is ON, D3 can be forward-biased depending on the load and source conditions. This diode sometimes ensures no back-feed to the source, so the voltage across it may be zero or near zero, as shown in Fig. 7c. When the MOSFET switch is

OFF, D3 is reverse-biased, carrying the voltage difference between the source and the inductor. The switching devices' states and the inductor's dynamics influence the voltage waveforms across the diodes. Diodes D1 and D2 primarily define the inductor's charging and discharging phases. The diode D3 often provides a path for circulating currents or acts as a protection diode to prevent back-feeding into the source. Turning our attention to the two diodes, namely D4 and D5, associated with the SC, their voltage stress can be seen in Figs. 7d-7e. This voltage stress is approximately -116 volts for both diodes.

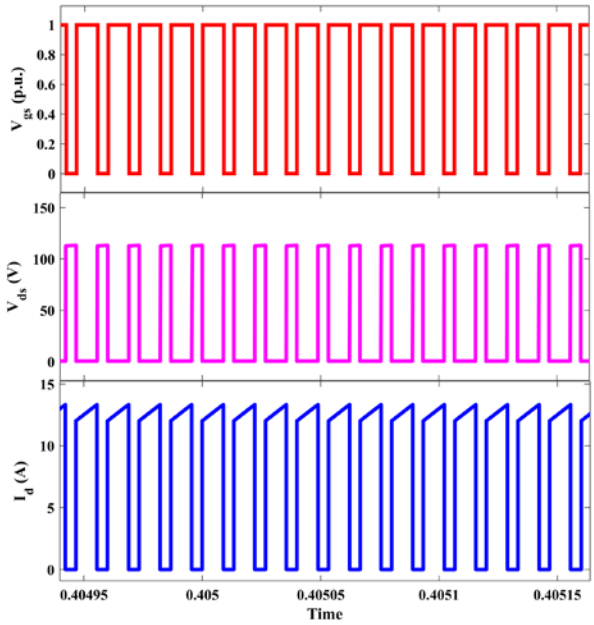

Fig. 6. Voltage and current waveforms; (a) Gate pulse; (b) MOSFET voltage stress; (c) MOSFET current stress

Regarding their operation relative to the MOSFET: When MOSFET is inactive (or in its off-state), both D4 and D5 diodes are conducting and contrarily, when MOSFET is active (or in its on-state), these diodes cease to conduct, as depicted in Figs. 7d-7e. Figure 8 visually represents the current waveforms for the inductors labelled as L1, L2, and L3. These inductors follow an operational pattern relative to MOSFET: They engage in a charging process when the MOSFET is active (on). When the MOSFET switches to its off state, these inductors begin discharging.

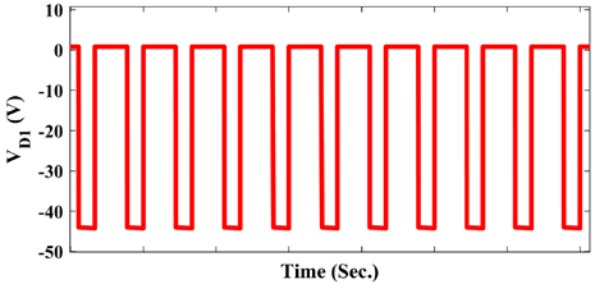

(a)

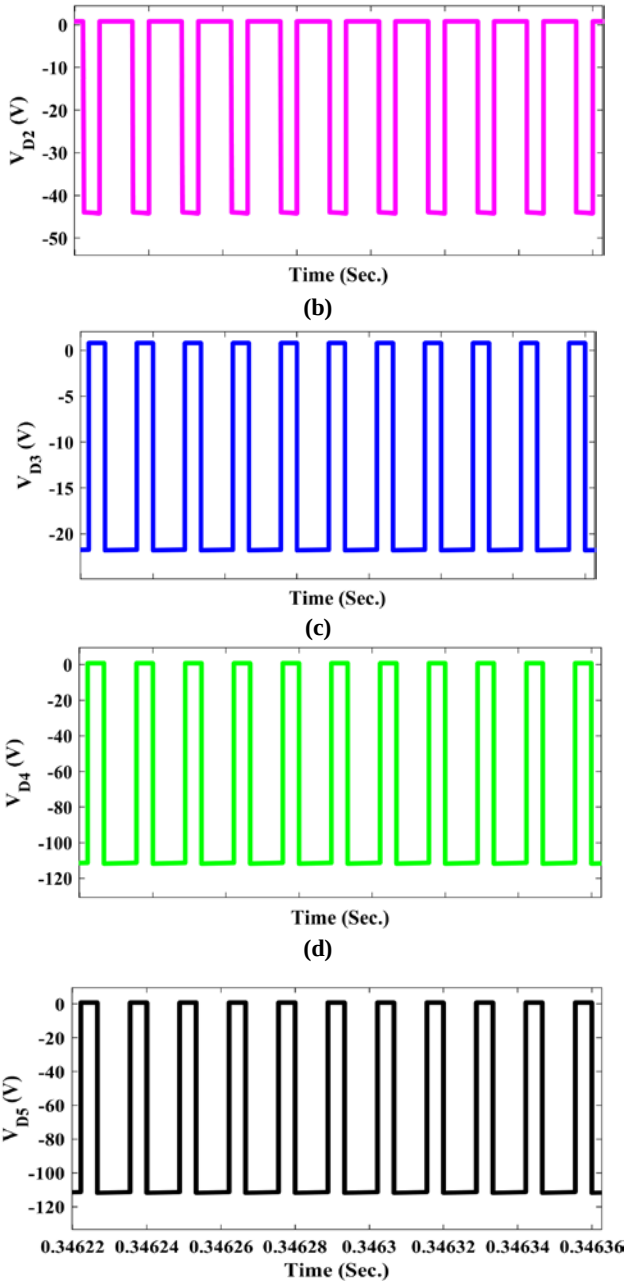

Fig. 7. Diode voltage waveforms; (a) V_{D1}, (b) V_{D2}, (c) V_{D3}, (d) V_{D4}, (e) V_{D5}

When MOSFET is ON, the source provides energy to charge up L1. Its current rises linearly due to the voltage applied from the source. The configuration suggests that there is a path for L2 to charge as well when MOSFET is ON. This is likely established by the diodes (D1, D2, and D3). One scenario is that D1 allows the current to flow into L2, charging it. As with L1, the current in L2 also ramps up linearly with respect to the applied voltage. During the ON-time of the switch, both inductors are being charged by the voltage source, and their currents increase. The slope of the current increase $\left(\frac{di}{dt}\right)$ is determined by the voltage across the inductor and its

inductance value according to the relation $V = L\frac{di}{dt}$. When MOSFET is turned OFF, L1's stored energy needs a path to release.

Depending on the diode orientations, the energy could either flow towards the output, transfer to L2, or combine both. L2 also starts discharging its energy. If L1's energy is not being transferred to L2, then L2 could be discharging its energy directly to the output through one of the diodes, likely D2 or D3. During the OFF-time, both inductors discharge their stored energy. The current waveform during this period would depend on various factors like the load, the diode orientations, and the amount of energy stored in each inductor. The current waveform showcases a linear ramp-up for L1 and L2 in a scenario where both inductors charge during the ON-time. When the switch is OFF, the current waveforms for the inductors would ramp down. The rate of this ramp-down, or the slope, would depend on the path taken by the current (which diodes are conducting) and the load conditions.

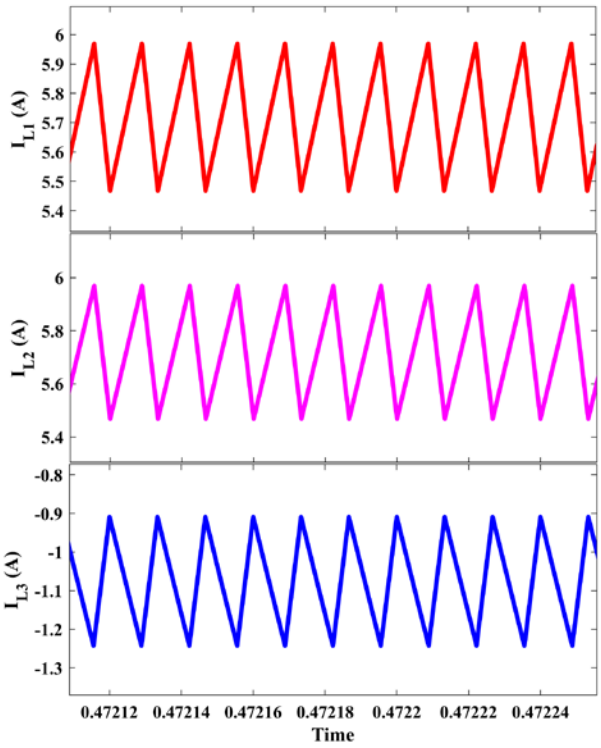

Fig. 8. Inductor current waveforms: (a) I_{L1}, (b) I_{L2}, (c) I_{L3}

The voltage waveforms associated with C1 and C2 are presented in Fig. 9. Notably, the capacitors undergo a charging process when the MOSFET is in an OFF state. Conversely, these capacitors discharge when the MOSFET enters its ON state. During charging, initially, if C1 starts at 0V (or a lower voltage level), its voltage begins to increase. The charging rate is determined by the on-state resistance of the MOSFET, including source, resistance, and the presence of those diodes.

The voltage across C1 increases until it reaches its maximum charge or until the MOSFET switches states. Similarly, C2 also charge, and the diodes influence its rate. The voltage across C1 and C2 decreases until it's completely discharged or until the MOSFET returns to the OFF state. It is also worth noting that, in actual circuits, other factors like parasitic capacitances, MOSFET gate charges, diode forward voltages, and so forth can also influence the waveform. The presence of diodes in a switched capacitor cell can significantly influence the behaviour of the capacitors, both in terms of charging and discharging.

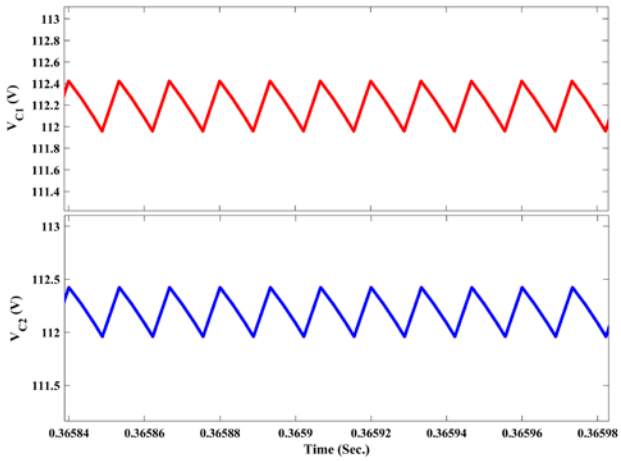

Fig. 9. Capacitor voltage waveforms; (a) V_{C1}, (b) V_{C2}

When the MOSFET is in the ON state, it is possible for a capacitor at a higher voltage to discharge into another capacitor at a lower voltage. A diode can prevent this undesired current flow, ensuring that capacitors don't unintentionally discharge into other parts of the circuit or other capacitors. The diodes can protect the capacitors from voltage spikes or transient behaviours, especially during the switching action of the MOSFET. By preventing reverse current flow, diodes can ensure that sudden voltage changes do not cause current spikes in undesired directions. The diode's forward resistance and the junction capacitance can influence the rate at which the capacitor charges or discharges. Therefore, the diodes in an SC cell primarily ensure unidirectional current flow and can prevent undesired interactions between capacitors and other elements during the switching phases. However, they also introduce certain challenges, such as voltage drops and potential thermal issues, which designers must consider. Since the proposed converter can operate in both boost and buck modes, the input voltage can be either greater than, less than, or equal to the desired output voltage. The input current waveform of the proposed converter is continuous, which means it does not drop to zero during any part of the switching cycle, similar to the traditional Cuk converter. This is a desirable feature in many applications because a continuous input current can reduce the stress on source components and reduce electromagnetic interference. The inductors on the input side, i.e., the SL cell, ensure the current waveform is continuous. However, the ripple in the input current is also

influenced by the value of this inductor and the frequency of operation. The input voltage and current waveforms are exhibited in Fig. 10 for an overarching understanding.

Figure 11 serves as a one-stop reference, capturing the output voltage, current, and power waveforms. It is a testament to the converter's overall efficiency and dynamic operation. The proposed SCSL-based Cuk converter showcases a delicate balance of design, efficiency, and performance, which can be comprehended deeply by examining its components and their dynamic interactions.

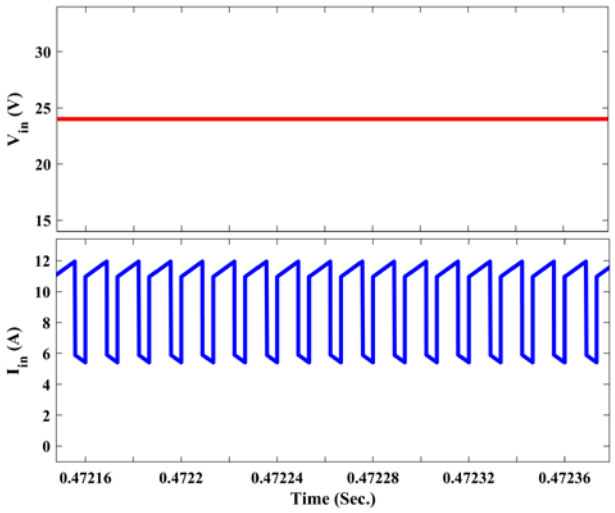

Fig. 10. Input voltage and current waveforms; (a) V_{in}, (b) I_{in}

The proposed converter's efficiency is computed after considering the distinct types of losses, each playing a unique role in the converter's overall performance. These losses are categorized into three main components: conduction losses, switching losses, and control losses[51]. The conduction losses occur due to the resistance semiconductor devices offer when in the conducting state. In other words, when current flows through the device, this intrinsic resistance dissipates power, leading to losses. This phenomenon is particularly observed in diodes and MOSFET when in an ON state. As semiconductors switch between their ON and OFF states, energy is lost. The control is losses associated with the circuits that govern the operation of the semiconductor devices. It includes the energy used by gate drivers, control logic circuits, and other auxiliary circuits that ensure the correct functioning of the semiconductor devices. While these losses might be comparatively smaller, they are still significant for the overall efficiency of the converter. It is crucial to emphasize that these types of losses are inherent to the operation of semiconductor devices. Therefore, any optimization or improvement in converter design should consider minimizing these losses to enhance overall efficiency. For a more comprehensive understanding and mathematical representation of these losses, Table 3 offers a detailed breakdown of each loss component, accompanied by its associated equation. Table 3 can serve as a valuable reference for those looking to delve deeper into the intricacies of converter inefficiencies.

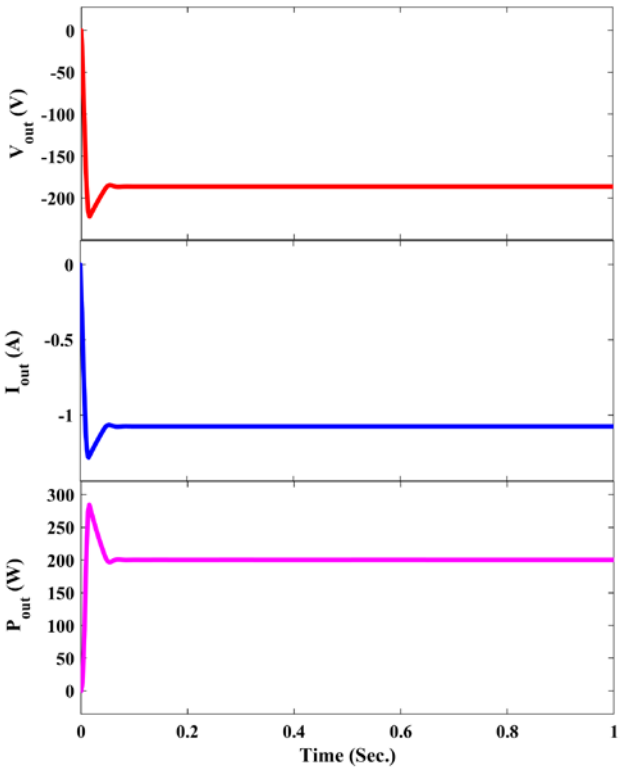

Fig. 11. Output side waveforms; ; (a) V_{out}, (b) I_{out}, (c) P_{out}

Table 3. Various losses associated with the proposed converter

Losses	Equation	Remarks
Switching Loss	$P_S = 5f_sC_{oss}(0.5V_{in} + V_{out})^2$	C_{oss} and C_d denote the output capacitance of the MOSFET and diodes, respectively.
	$P_D = 5f_sC_d(0.5V_{in} + V_{out})^2$	
Conduction Loss	$P_S = i_d^2R_{ds-ON}D$	R_{ds-ON} and R_f denote the MOSFET and diodes on-state resistance and V_f denotes the forward voltage drop.
	$P_D = (V_f i_d + I_d^2R_f)(1 - D)$	
Passive Devices	$R_{L1} = R_{1dc}\left(\frac{DT_sV_{in}}{L_1}\right)^2$	

	$R_{L2} = R_{2dc}\left(\frac{DT_sV_{in}}{L_2}\right)^2$	Losses in each inductor are based on the DC resistance. Due to the small effective resistances, the losses in the capacitors of the SC are ignored.
	$R_{L3} = R_{3dc}\left(\frac{DT_sV_{out}}{L_3}\right)^2$	
Control Loss	$P_{gates} = Q_gV_{gs}f_s$	Q_g denotes the gate charge of the MOSFET.

The effectiveness of the proposed SCSL-based Cuk converter is being evaluated in comparison to the traditional Cuk converter and two modified Cuk converters presented in the literature, as depicted in Fig. 12. The performance computation encompasses all loss components, encompassing control, switching, and conduction losses. The efficacy is also determined by calculating load current variations ranging from 10% to 125% of the rated capacity. According to the data presented in Fig. 11, it can be observed that the efficiency of the suggested converter surpasses that of the Cuk and its other modified converters when the load is augmented. The efficacy of the suggested topology is approximately 91.5% under full load, whereas the Cuk converter achieves an efficacy of 86% under similar rated parameters.

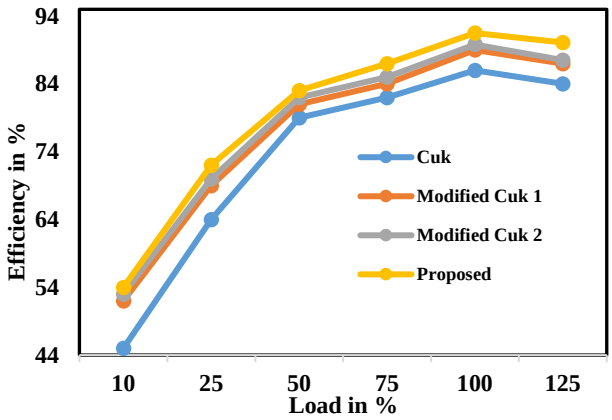

Fig. 12. Efficiency curve of all the converter topologies

The efficiency of a system tends to improve when the input voltage increases due to a drop in input current. Consequently, this reduction in input current leads to decreased conduction losses of power switches. Upon analyzing the results presented and discussed previously, it is concluded that the suggested SCSL-based Cuk converter exhibits several favourable attributes compared to the traditional Cuk converter. These include a decrease in the voltage of the coupling capacitor, enhanced effectiveness, and a quicker transient response.

5. Conclusions

The present research has achieved a milestone in developing a new Cuk converter topology that boasts a notable high voltage gain while concurrently minimizing the stress on the active switch. An outstanding feature of this advancement is the ability to attain this high voltage gain without resorting to conventional mechanisms like transformers, coupled inductors, or extreme duty cycles. When delving deeper into the operational modalities, it was observed that the proposed converter predominantly functions in the continuous conduction mode. This mode ensures a seamless flow of energy, thereby preventing erratic energy pulses, which can sometimes affect the efficiency of power converters. In terms of regulation, the proposed converter capitalizes on the Pulse Width Modulation (PWM) technique. It operates at a stable frequency, ensuring the consistency of the output irrespective of variable input conditions. For clearer demarcation of the benefits of this new topology, the research contrasted the proposed converter against the conventional Cuk converter and several of its other variants. This comparative assessment underlined several merits of the newly introduced converter. Chief among the advantages is the elevated voltage gain, a crucial metric in power electronics. Furthermore, the new design ensures a remarkably low voltage stress. This reduction in voltage stress is not merely an academic achievement but has practical ramifications. It paves the way for selecting a semiconductor switch with a lower voltage capacity and a reduced $R_{ds\text{-}ON}$ value. This, in turn, augments the converter's efficiency and reliability. Other remarkable features include the continuous nature of both the input and output current, which enhances energy flow stability. Furthermore, the topology is characterized by the use of a singular switch. This is cost-effective and simplifies the overall design, making it more amenable to practical applications. The design outperforms many of its peers on the efficiency frontier, while its simplicity ensures ease of implementation. From an analytical standpoint, the research delved deep into the steady-state analysis of voltage gain, elucidating the intricacies involved in the process. The simulation outcomes, carried out using the MATLAB/SIMULINK platform, are in robust agreement with the established operational modes and the mathematical equations derived during the study. This congruence between theory and simulated practice adds another layer of credibility to the proposed topology.

While this research has provided a strong foundation for developing a new Cuk converter topology, there is a potential for further exploration and refinement. Future

endeavours could:

- Probe into the converter's performance under different load conditions, evaluating its robustness and adaptability.
- Investigate the scalability of this design for larger industrial applications, ensuring its relevance in diverse scenarios.
- Exploring advanced control strategies, such as predictive control or adaptive control, to further enhance the performance, efficiency, and reliability of the converter under varying operating conditions.
- Investigating the converter's potential in renewable energy applications, particularly in solar and wind energy systems, where its high efficiency and voltage regulation capabilities can be pivotal.
- Delving deeper into thermal management solutions to ensure optimal operation of the converter, especially in high-power or high-temperature environments.
- Develop modular converter designs that can be easily scaled up or down based on the specific power requirements of different applications.
- Researching advanced filtering and shielding techniques to further reduce electromagnetic interference, especially at higher switching frequencies.
- Exploring the converter's compatibility and performance in smart grid environments, focusing on aspects like remote monitoring, control, and predictive maintenance using IoT technologies.
- Investigating the use of novel materials, such as wide-bandgap semiconductors, to enhance the converter's efficiency, reduce losses, and extend its operational lifespan.

The journey has been promising, and with continued research, there is immense potential for this Cuk converter topology to revolutionize the landscape of power electronics.

Acknowledgements

The authors thank the anonymous reviewers for their insightful criticism that helped to strengthen the paper.

References

1) M. Premkumar, K. Karthick, R. Sowmya, A comparative study and analysis on conventional solar PV based DC-DC converters and MPPT techniques, Indonesian Journal of Electrical Engineering and Computer Science. (2018). https://doi.org/10.11591/ijeecs.v11.i3.pp831-838.
2) M. Premkumar, T.R. Sumithira, Design and Implementation of New Topology for Nonisolated DC?DC Microconverter with Effective Clamping Circuit, Journal of Circuits, Systems and Computers. (2018). https://doi.org/10.1142/S0218126619500828.
3) B.S. Revathi, P. Mahalingam, F. Gonzalez-longatt, Interleaved high gain DC-DC converter for integrating solar PV source to DC bus, Solar Energy. 188 (2019) 924–934. https://doi.org/10.1016/j.solener.2019.06.072.
4) B.P. Baddipadiga, M. Ferdowsi, A High-Voltage-Gain DC-DC Converter Based on Modified Dickson Charge Pump Voltage Multiplier, IEEE Trans Power Electron. 32 (2017) 7707–7715. https://doi.org/10.1109/TPEL.2016.2594016.
5) C. Harsito, M.R.A. Putra, D.A. Purba, T. Triyono, Mini Review of Thermoelectric and their Potential Applications as Coolant in Electric Vehicles to Improve System Efficiency, Evergreen. 10 (2023) 469–479. https://doi.org/10.5109/6782150.
6) M.M. Rahman, S. Saha, M.Z.H. Majumder, T.T. Suki, M.H. Rahman, F. Akter, M.A.S. Haque, M.K. Hossain, Energy Conservation of Smart Grid System Using Voltage Reduction Technique and Its Challenges, Evergreen. 9 (2022) 924–938. https://doi.org/10.5109/6622879.
7) S.S. Mendu, P. Appikonda, A.K. Emadabathuni, N. Koritala, Techno-economic comparative analysis between grid-connected and stand-alone integrated energy systems for an educational institute, Evergreen. 7 (2020) 382–395. https://doi.org/10.5109/4068616.
8) P. Manoharan, U. Subramaniam, T.S. Babu, S. Padmanaban, J.B. Holm-Nielsen, M. Mitolo, S. Ravichandran, Improved perturb and observation maximum power point tracking technique for solar photovoltaic power generation systems, IEEE Syst J. 15 (2021) 3024–3035. https://doi.org/10.1109/JSYST.2020.3003255.
9) M. Premkumar, C. Kumar, R. Sowmya, Analysis and implementation of high-performance DC-DC step-up converter for multilevel boost structure, Front Energy Res. 7 (2019). https://doi.org/10.3389/fenrg.2019.00149.
10) A.K. Bohre, Y. Sawle, V.K. Jadoun, A. Agarwal, Assessment of Techno-Socio-Economic Performances of Distribution Network with Optimal Planning of Multiple DGs, Evergreen. 10 (2023) 1106–1112. https://doi.org/10.5109/6793670.
11) R. Kumar, A. Agarwal, Space Vector Modulation for Nine-Switch Converter Employing Three Phase Loads, Evergreen. 10 (2023) 1034–1040. https://doi.org/10.5109/6793659.
12) G.S. Reddy, M. Premkumar, S. Ravi, L. Abualigah, An intelligent converter and controller for electric vehicle drives utilizing grid and stand-alone solar photovoltaic power generation systems, International Journal of Applied Power Engineering (IJAPE). 12 (2023) 255–276. https://doi.org/10.11591/IJAPE.V12.I3.PP255-276.
13) A. Amir, A. Amir, H.S. Che, A. Elkhateb, N.A. Rahim, Comparative analysis of high voltage gain

DC-DC converter topologies for photovoltaic systems, Renew Energy. 136 (2019) 1147–1163. https://doi.org/10.1016/J.RENENE.2018.09.089.
14) M. Premkumar, C. Ramakrishnan, C. Kumar, R. Sowmya, T.R. Sumithira, P. Jangir, An Improved Quasi-Z-Source Boost DC-DC Converter Using Single-Stage Switched-Inductor Boosting Technique, Machines 2022, Vol. 10, Page 669. 10 (2022) 669. https://doi.org/10.3390/MACHINES10080669.
15) S. Hamkari, M. Moradzadeh, E. Zamiri, M. Nasiri, S.H. Hosseini, A Novel Switched Capacitor High Step-up dc / dc Converter Using a Coupled Inductor with its Generalized Structure, 17 (2017) 579–589.
16) S. Jaisiva, C. Kumar, K. Viji, M. Premkumar, M. Lakshmanan, V. Jayakumar, Enhancement of Voltage Conversion Ratio using DC-DC Boost Converter with Coat Circuit, 2022 3rd International Conference on Communication, Computing and Industry 4.0 (C2I4). (2022) 1–5. https://doi.org/10.1109/C2I456876.2022.10051308.
17) N. Kumari, S.K. Singh, S. Kumar, MATLAB-Based Simulation Analysis of the Partial Shading at Different Locations on Series-Parallel PV Array Configuration, Evergreen. 9 (2022) 1126–1139. https://doi.org/10.5109/6625724.
18) M.W. AlShaar, Z. Al-Omari, W. Emar, M. Alnsour, G. Abu-Rumman, Application of PV-Thermal Array for Pumping Irrigation Water as an Alternative to PV in Ghor Al-Safi, Jordan: A case study, Evergreen. 9 (2022) 1140–1150. https://doi.org/10.5109/6625725.
19) A. Abdalrahman, W. Zhuang, A Survey on PEV Charging Infrastructure: Impact Assessment and Planning, Energies 2017, Vol. 10, Page 1650. 10 (2017) 1650. https://doi.org/10.3390/EN10101650.
20) A.M.S.S. Andrade, E. Mattos, L. Schuch, H.L. Hey, M.L. Da Silva Martins, Synthesis and Comparative Analysis of Very High Step-Up DC-DC Converters Adopting Coupled-Inductor and Voltage Multiplier Cells, IEEE Trans Power Electron. 33 (2018) 5880–5897. https://doi.org/10.1109/TPEL.2017.2742900.
21) G.A. Putrus, P. Suwanapingkarl, D. Johnston, E.C. Bentley, M. Narayana, Impact of electric vehicles on power distribution networks, 5th IEEE Vehicle Power and Propulsion Conference, VPPC '09. (2009) 827–831. https://doi.org/10.1109/VPPC.2009.5289760.
22) T.A. Stanley Raja, C. Kumar, M. Premkumar, Novel Multilevel Inverter using Switched Capacitor unit with Voltage Boosting feature for EV Applications, 2022 International Conference on Disruptive Technologies for Multi-Disciplinary Research and Applications (CENTCON). (2022) 157–161. https://doi.org/10.1109/CENTCON56610.2022.10051339.
23) B. Singh, B.N. Singh, A. Chandra, K. Al-Haddad, A. Pandey, D.P. Kothari, A review of single-phase improved power quality AC-DC converters, IEEE Transactions on Industrial Electronics. 50 (2003) 962–981. https://doi.org/10.1109/TIE.2003.817609.
24) R. Oruganti, R. Srinivasan, Single phase power factor correction - A review, Sadhana. 22 (1997) 753–780. https://doi.org/10.1007/BF02745844/METRICS.
25) G.I. Kishore, M. Premkumar, R.K. Tripathi, C.S. Nalamati, A Novel Single Switch High Gain DC-DC Converter Topology for Renewable Energy Systems, Energy Engineering. 118 (2020) 199–209. https://doi.org/10.32604/EE.2021.014079.
26) M. Madigan, R. Erickson, E. Ismail, Integrated High quality rectifier-regulators, PESC Record - IEEE Annual Power Electronics Specialists Conference. (1992) 1043–1051. https://doi.org/10.1109/PESC.1992.254769.
27) R. Redl, L. Balogh, Design considerations for single-stage isolated power-factor-corrected power supplies with fast regulation of the output voltage, Conference Proceedings - IEEE Applied Power Electronics Conference and Exposition - APEC. 1 (1995) 454–458. https://doi.org/10.1109/APEC.1995.468987.
28) H.M. Maheri, S. Member, E. Babaei, S. Member, High Step-up DC-DC Converter with Minimum Output Voltage Ripple, 0046 (2017). https://doi.org/10.1109/TIE.2017.2652395.
29) E. Pazouki, S. Member, Y. Sozer, Fault Diagnosis and Fault Tolerant Operation of Non-Isolated DC-DC Converter, 9994 (2017). https://doi.org/10.1109/TIA.2017.2751547.
30) A. Amir, A. Amir, H. Seng, A. Elkhateb, N. Abd, Comparative analysis of high voltage gain DC-DC converter topologies for photovoltaic systems, Renew Energy. 136 (2019) 1147–1163. https://doi.org/10.1016/j.renene.2018.09.089.
31) E.H. Ismail, M.A. Al-Saffar, A.J. Sabzali, A.A. Fardoun, A family of single-switch PWM converters with high step-up conversion ratio, IEEE Transactions on Circuits and Systems I: Regular Papers. 55 (2008) 1159–1171. https://doi.org/10.1109/TCSI.2008.916427.
32) X. Wei, C. Luo, H. Nan, Y. Wang, A Simple Structure of Zero-Voltage Switching (ZVS) and Zero-Current Switching (ZCS) Buck Converter with Coupled Inductor, Journal of Power Electronics. 15 (2015) 1480–1488. https://doi.org/10.6113/JPE.2015.15.6.1480.
33) Y.K. Tai, K.I. Hwu, A Novel ZVS/ZCS Push-Pull LC Resonant DC-DC Converter for Energy Sources, Energies 2023, Vol. 16, Page 2892. 16 (2023) 2892. https://doi.org/10.3390/EN16062892.
34) M. Premkumar, U. Subramaniam, H. Haes Alhelou, P. Siano, Design and Development of Non-Isolated Modified SEPIC DC-DC Converter Topology for High-Step-Up Applications: Investigation and Hardware Implementation, Energies (Basel). 13 (2020) 3960. https://doi.org/10.3390/en13153960.

35) M. Premkumar, C. Kumar, A. Anbarasan, R. Sowmya, A novel non-isolated high step-up DC–DC boost converter using single switch for renewable energy systems, Electrical Engineering. 102 (2020) 811–829. https://doi.org/10.1007/S00202-019-00904-8/METRICS.
36) D. Buvana, R. Jayashree, ANFIS Controller Based Cascaded Non-Isolated Bi-Directional DC-DC Converter, Journal OfCircuits, Systems, and Computers. (2018). https://doi.org/10.1142/S0218126619500014.
37) J. Wang, B. Wang, L. Zhang, J. Wang, N.I. Shchurov, B. V. Malozyomov, Review of bidirectional DC–DC converter topologies for hybrid energy storage system of new energy vehicles, Green Energy and Intelligent Transportation. 1 (2022) 100010. https://doi.org/10.1016/J.GEITS.2022.100010.
38) H. Gholizadeh, S.A. Gorji, E. Afjei, D. Sera, Design and Implementation of a New Cuk-Based Step-Up DC–DC Converter, Energies 2021, Vol. 14, Page 6975. 14 (2021) 6975. https://doi.org/10.3390/EN14216975.
39) Y. Almalaq, M. Matin, Three Topologies of a Non-Isolated High Gain Switched-Inductor Switched-Capacitor Step-Up Cuk Converter for Renewable Energy Applications, Electronics 2018, Vol. 7, Page 94. 7 (2018) 94. https://doi.org/10.3390/ELECTRONICS7060094.
40) B.R. Ananthapadmanabha, R. Maurya, S.R. Arya, Improved Power Quality Switched Inductor Cuk Converter for Battery Charging Applications, IEEE Trans Power Electron. 33 (2018) 9412–9423. https://doi.org/10.1109/TPEL.2018.2797005.
41) A. Ajami, H. Ardi, A. Farakhor, Design, analysis and implementation of a buck–boost DC/DC converter, IET Power Electronics. 7 (2014) 2902–2913. https://doi.org/10.1049/IET-PEL.2013.0874.
42) J.G. Baek, T. Nomiyama, S. Park, Y.H. Jung, D. Kim, J. Han, J.S. Bang, Y. Lee, I.H. Kim, J.S. Paek, J. Lee, T.B. Cho, A Voltage-Tolerant Three-Level Buck-Boost DC-DC Converter with Continuous Transfer Current and Flying Capacitor Soft Charger Achieving 96.8% Power Efficiency and 0.87μs/V DVS Rate, Dig Tech Pap IEEE Int Solid State Circuits Conf. 2020-February (2020) 202–204. https://doi.org/10.1109/ISSCC19947.2020.9063105.
43) P.K. Maroti, S. Padmanaban, P. Wheeler, F. Blaabjerg, M. Rivera, Modified high voltage conversion inverting cuk DC-DC converter for renewable energy application, Proceedings - 2017 IEEE Southern Power Electronics Conference, SPEC 2017. 2018-January (2018) 1–5. https://doi.org/10.1109/SPEC.2017.8333675.
44) M. Shaabani, A. Mirzaei, M. Rezvanyvardom, F. Khosravi, S.A. Gorji, A Hybrid Switched-Inductor/Switched-Capacitor DC-DC Converter with High Voltage Gain Using a Single Switch for Photovoltaic Application, Energies 2023, Vol. 16, Page 5524. 16 (2023) 5524. https://doi.org/10.3390/EN16145524.
45) Y. Pola, S.K. Nibhanupudi, N. Karra, P.N. Meghavath, Switched Inductor Based DC-DC Converters for Electric vehicles: A Comprehensive Review, INDICON 2022 - 2022 IEEE 19th India Council International Conference. (2022). https://doi.org/10.1109/INDICON56171.2022.10039984.
46) X. Wu, J. Wang, Y. Zhang, Z. Liu, Switched-capacitor-based high-gain DC–DC converter for fuel cell vehicle powertrain, Journal of Power Electronics. 22 (2022) 557–568. https://doi.org/10.1007/S43236-022-00388-Z/METRICS.
47) A.F. de Souza, F.L. Tofoli, E.R. Ribeiro, Switched Capacitor DC-DC Converters: A Survey on the Main Topologies, Design Characteristics, and Applications, Energies 2021, Vol. 14, Page 2231. 14 (2021) 2231. https://doi.org/10.3390/EN14082231.
48) D. Zhou, A. Pietkiewicz, S. Ćuk, A three-Switch high-Voltage converter, IEEE Trans Power Electron. 14 (1999) 177–183. https://doi.org/10.1109/63.737606.
49) S. Ćuk, R. Middlebrook, A general unified approach to modelling switching DC-tO-DC converters in discontinuous conduction mode, PESC Record - IEEE Annual Power Electronics Specialists Conference. 2015-March (2015) 36–57. https://doi.org/10.1109/PESC.1977.7070802.
50) H. Liu, H. Hu, H. Wu, Y. Xing, I. Batarseh, Overview of High-Step-Up Coupled-Inductor Boost Converters, IEEE J Emerg Sel Top Power Electron. 4 (2016) 689–704. https://doi.org/10.1109/JESTPE.2016.2532930.
51) K.A. Mahafzah, A.Q. Al-Shetwi, M.A. Hannan, T.S. Babu, N. Nwulu, A New Cuk-Based DC-DC Converter with Improved Efficiency and Lower Rated Voltage of Coupling Capacitor, Sustainability 2023, Vol. 15, Page 8515. 15 (2023) 8515. https://doi.org/10.3390/SU15118515.